Macrospin behavior and superparamagnetism in (Ga,Mn)As nanodots

J.-P. Adam,[1] S. Rohart,[1,*] J. Ferré,[1] A. Mougin,[1] N. Vernier,[1] L. Thevenard,[2] A. Lemaître,[2] G. Faini,[2] and F. Glas[2]
[1]*Laboratoire de Physique des Solides, CNRS, Université Paris Sud, UMR 8502, F-91405 Orsay Cedex, France*
[2]*Laboratoire de Photonique et de Nanostructures, CNRS, UPR 20, F-91460 Marcoussis, France*
(Received 13 July 2009; revised manuscript received 10 September 2009; published 9 October 2009)

An array of small independent and quasimonodisperse nanodots of the dilute magnetic semiconductor (Ga,Mn)As with out-of-plane easy axis has been patterned by electronic lithography and ion-beam etching from a strained epitaxial film. The thermal dependence ($2<T<120$ K) of the field-induced magnetic loops, coercivity, and anisotropy of the nanodots, have been measured by sensitive magneto-optical magnetometry. Below the superparamagnetic blocking temperature T_B, all results are consistent with a quasicoherent thermally activated and field-induced spin-rotation process. In spite of the nonconventional nature of the ferromagnetism mediated by holes and of the high dilution in manganese ions, T_B is well accounted for by the usual Néel-Brown model.

DOI: 10.1103/PhysRevB.80.155313 PACS number(s): 75.50.Pp, 75.75.+a, 75.20.−g

I. INTRODUCTION

When the size of small magnetic particles is reduced down to some tens of nanometers, thermal fluctuations destabilize the magnetization direction and favor a superparamagnetic state.[1,2] This transition occurs at the so-called blocking temperature, T_B, when the sampling rate t equals the thermal fluctuation rate τ of the magnetization direction. This physical limit restricts the use of nanoparticles for application to ultrahigh-density magnetic recording.[3] The simplest description of superparamagnetism, proposed by Néel-Brown,[1,2] relies on a coherent reversal of the magnetization, that behaves as a single giant spin (or macrospin) with a fluctuation rate given by $\tau=\tau_0 \exp(K_{\mathrm{eff}}V/k_BT)$ (K_{eff} being the effective anisotropy constant, which accounts here for magnetocrystalline and shape anisotropy, V the particle volume and τ_0 the inverse of the attempt frequency). The validity of this law was convincingly tested at low temperature on a single metallic particle,[4] and slow fluctuations in spin orientation were observed in the vicinity of T_B.[4,5] Besides, measurements carried out on large assemblies of nanoelements, showing distributions of structural, morphological, and magnetic parameters, restrain from interpreting most data.[6–8] Too often, nanoelements previously studied[9–11] are large compared to the exchange length Λ so that magnetization reversal proceeds by a noncoherent mechanism. In metallic particles, Λ is so small (about 5–10 nm) that only bottom-up preparation methods lead to particles of diameter D satisfying the condition $D \lesssim \Lambda$. The favorite physical preparation method is crystal growth on well-chosen metallic templates[12,13] and it is only in rare cases[13,14] that reliable information can be obtained from controlled narrow distributions of morphological and magnetic parameters. Eventually, trustworthy interpretation requires a separation between the nanoparticles large enough to rule out interactions between them.

In spite of their large interest for memory and spintronic applications, magnetization-reversal processes in diluted magnetic semiconductor (DMS) nanoelements have not been investigated so far. We propose here to test the macrospin model in diluted (Ga,Mn)As single-domain nanodots with out-of-plane easy axis and check the validity of the Néel-Brown law for deducing T_B in such nonmetallic ferromagnet. (Ga,Mn)As is the archetypal example of DMS, showing a high Curie temperature[15] where the long-range ferromagnetic interactions are mediated by hole carriers. The onset of superparamagnetism of nanosized flat (Ga,Mn)As nanodots with in-plane anisotropy has been recently proved.[16] However, the results did not allow testing the validity of the Néel-Brown model as the size distribution was large and the in-plane anisotropy rather complicated. In this paper, we focus on a very well-defined system (narrow size distribution, out-of-plane anisotropy) which simplifies interpretations and allows proving that the Néel-Brown model can really be applied to this material.

II. EXPERIMENTAL DETAILS

Starting from a strained (Ga,Mn)As epitaxial film with perpendicular anisotropy, patterning and etching processes were used to define confined DMS nanodots. The virgin $Ga_{0.93}Mn_{0.07}As$ (50-nm-thick) film was grown by molecular-beam epitaxy on a gradient In-doped $Ga_xIn_{1-x}As$ buffer layer deposited on a GaAs (001) substrate.[17] The indium concentration gradient was essentially used to reduce the emergent dislocation density in the (Ga,Mn)As film. The lattice mismatch between (Ga,Mn)As and (Ga,In)As induces tensile strains in the (Ga,Mn)As layer that favor perpendicular magnetic anisotropy.[18] In order to reduce the number of Mn interstitial atoms, the film was annealed at 250 °C during one hour. After this treatment, the Curie temperature of the (Ga,Mn)As film was of 116 K.

Several arrays 80 μm$\times$50 μm wide of nanodots with diameter ranging from 33 to 230 nm were patterned by electron-beam lithography and ion-beam etching through a Ti mask. After processing, the region between dots was etched down to the (Ga,Mn)As/(Ga,In)As interface and the (Ga,Mn)As dot thickness was reduced to $h=28$ nm as compared to 50 nm for the virgin film. Furthermore, a 340 μm$\times$340 μm square and 28-nm-thick (Ga,Mn)As pad was preserved for the purpose of comparing nanodots and

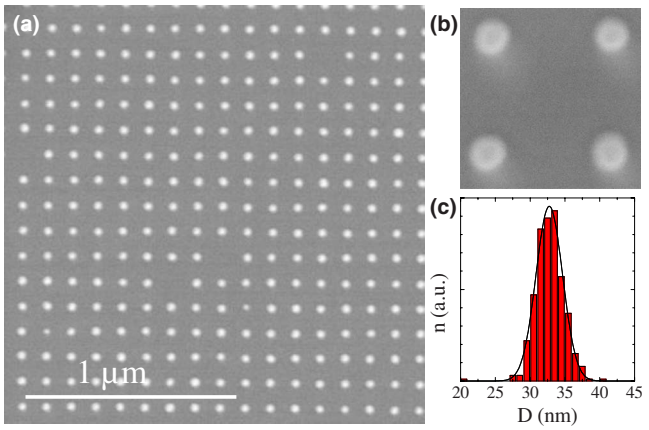

FIG. 1. (Color online) (a) 2×2 μm^2 SEM-FEG image of the $Ga_{0.93}Mn_{0.07}As$ dot array. (b) 170×170 nm^2 zoom. (c) Diameter distribution obtained from the SEM-FEG images.

thin-film magnetic properties after the same patterning process.

The main investigations in this paper concern the array of $D=33$ nm cylindrical nanodots [Figs. 1(a) and 1(b)]. Because of the weak magnetization in (Ga,Mn)As, the nanodot periodicity, which is 115 nm, is large enough to neglect interdot magnetostatic coupling[6] (in the other arrays of wider nanodots, the spacing was always larger than 150 nm, which is still sufficient to neglect interdot magnetostatic interactions). The diameter distribution estimated from field-emission gun scanning electron microscopy (SEM-FEG) images of an assembly of 460 dots [Fig. 1(c)] is nearly Gaussian, centered on 33 nm, with a full width at half maximum of 4.4 nm. Their height, $h=28\pm2$ nm was deduced from atomic force microscopy measurements on the widest ($D\approx230$ nm) dots to limit convolution effects. This corresponds to a mean nanodot volume $V=(2.4\pm0.7)\times10^4$ nm^3, i.e., about $3-4\times10^4$ Mn atoms per nanodot. The absence of magnetism in etched regions of the sample was confirmed by polar magneto-optical Kerr effect (PMOKE) microscopy. Note that, from a geometric point of view, a rather monodisperse nanoelements assembly is obtained as compared to most earlier studies on metallic dot arrays.[14]

When patterning the magnetic film in nanoelements, structural relaxation may change the magnetic parameters. In particular, as the perpendicular magnetic anisotropy is induced by the tensile strain imposed by the (In,Ga)As buffer, if relaxation occurs in the nanodots, it may cause a decrease in the anisotropy constant K_{eff}. Indeed, according to mean-field calculations from Dietl *et al.*,[18] a highly doped unstrained (Ga,Mn)As epilayer can only sustain weak perpendicular magnetic anisotropy. On the one hand, numerical elasticity calculations using the finite element package COMSOL (Ref. 19) show that the deep etching allows to relax significantly the strains inside each (Ga,Mn)As nanodot. The tensile stress affects the (Ga,Mn)As lattice only close to the (Ga,In)As/(Ga,Mn)As interface so that the strain vanishes rapidly within 4 nm inside the dot. This implies that the tensile strain-induced perpendicular anisotropy in nanodots might be reduced after patterning, as compared to that prevailing in the virgin film.[17] On the other hand, the isotropic

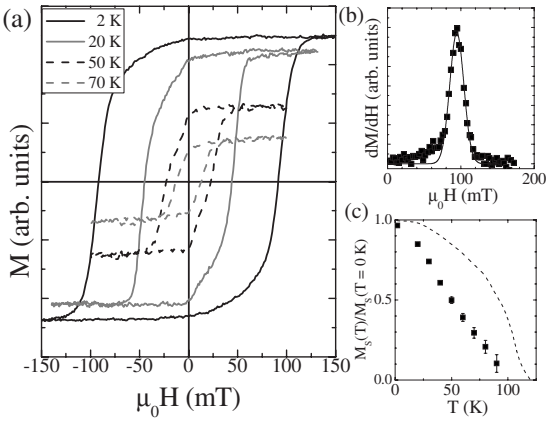

FIG. 2. (a) Magneto-optical PDCR hysteresis loops measured at different temperatures on the $D=33$ nm nanodot array. The $T=2$ K loop was averaged 40 times while at other temperatures, averaging was done on only ten loops. The field sweeping rate was 136 mT/s. (b) Derivative of the 2 K hysteresis loop versus H that allows determining the coercive-field distribution (Gaussian fit). The deviation at low field does not correspond to the switching field but to a reversible part in the hysteresis loop, which is not taken into account in the distribution. (c) Variation in the dot magnetization versus temperature (the dotted line corresponds to the reference-pad magnetization).

($h=28$ nm, $D=33$ nm) nanodot shape reduces the shape planar anisotropy as compared to the virgin film, which causes a slight increase in K_{eff}. In the following, the magnetic properties, and the above discussion, are addressed in more details.

III. EXPERIMENTS AND ANALYSIS

Magneto-optical investigations of the 33-nm-diameter nanodot array and of the reference pad have been performed from $T=2$ K up to 120 K. A small diaphragm (diameter 200 μm) was positioned just above the selected nanodot array. The estimated spot diameter of the focused HeNe laser ($\lambda=632.8$ nm) was also 200 μm. The light power at the sample location was then weaker than 50 μW, which strongly limits heating and possible photoinduced magnetic effects.[20] The perpendicular magnetization component has been measured by PMOKE, more precisely using the polar differential circular reflection (PDCR) that is the counterpart of magnetic circular dichroism in light transmission. Hysteresis loops were measured at several temperatures on the 33-nm-diameter dot array (Fig. 2). Informations relative to the thermal dependence of the saturation magnetization M_S, remnant magnetization M_R, coercive field H_C, and critical temperature have been deduced from PDCR hysteresis loops in a field applied perpendicular to the film plane.

In metallic systems, the blocking temperature is much smaller than the Curie temperature, which allows considering the magnetization and the anisotropy field as constants for temperatures below T_B. Here in contrast, due to the low T_C, the temperature dependences of the saturation magnetization, M_S, and of the effective anisotropy constant K_{eff} have to be determined and taken into account.

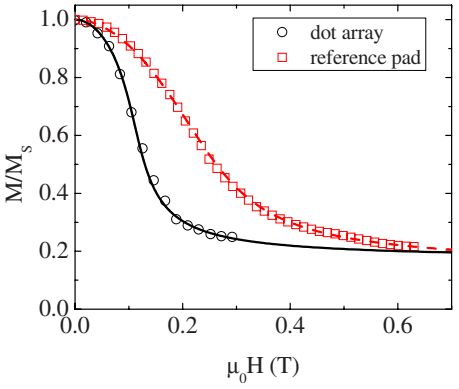

FIG. 3. (Color online) Anisotropy determination in the nanodot array (circles) and the reference pad (squares). The out-of-plane magnetization was measured with PMOKE while the magnetic field was aligned at $\alpha=10°$ from the basal film plane. In high field, the magnetization converges to $M/M_S=\sin\alpha$ and in zero field the magnetization is perfectly out of plane ($M/M_S=1$). The measurements are fitted with a coherent rotation model, which allows determining the anisotropy field (Ref. 22).

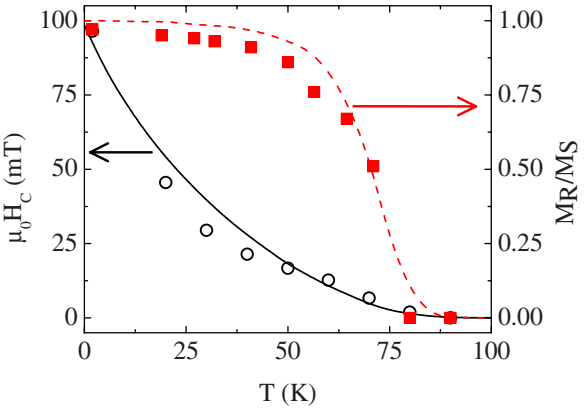

FIG. 4. (Color online) Temperature variation in remnant magnetization (filled squares) and coercive field (open circles) for the 33-nm-diameter nanodot array. The dots correspond to the experimental data while the lines correspond to the simulations (see text). Both sets of data are fitted using the same nonadjustable parameters determined from independent experiments.

The variation in M_S in the reference pad and in the nanodot array [see Fig. 2(c)] has been determined from the magneto-optical measurements in a saturating field [as shown in Fig. 2(a), for every loop, the maximum magnetic field was large enough to observe a clear saturation of the nanodot loops and to obtain a good accuracy on M_S; only at the highest temperatures, decreased signal-to-noise ratio, mechanical instabilities in large field and superparamagnetic effects make this determination less accurate as shown by the error bars]. As PMOKE only gives access to relative variations, we have assumed that the absolute value at $T=2$ K was the same as for the nonprocessed film ($\mu_0 M_S=42$ mT).[21] The reference-pad magnetization is found to decrease with temperature slightly more rapidly than a Brillouin law previously found for a virgin film.[17] This behavior is presumably linked to the fact that M_S is quite sensitive to the distribution of film properties. However, the Curie temperature $T_C=(111\pm1)$ K of the reference pad is not much reduced when compared to $T_C=116$ K for the virgin film. In the case of the nanodots, the variation is rather different and M_s decreases more rapidly than for the reference pad [see Fig. 2(c)].

The anisotropy field H_{eff} and the corresponding anisotropy constant K_{eff} have been experimentally determined on both nanodot array and reference pad. Following the procedure described in Ref. 22, the out-of-plane magnetization was measured while the magnetic field was essentially applied in the film plane (more precisely a well-defined angle of 10° from the basal film plane was used in order to work on a single magnetic domain). The reversible part of the curve is then fitted using the Stoner-Wohlfarth Hamiltonian, which supposes a coherent rotation (see Fig. 3). This allows a direct determination of H_{eff} at any temperature. The anisotropy constant is then deduced as $K_{\text{eff}}=\mu_0 M_S H_{\text{eff}}/2$. At 2 K the anisotropy field was measured to be 190 and 109 mT, respectively, on the reference pad and on the 33-nm-diameter nanodot array. The nanodot anisotropy field is much smaller than that of the reference pad, as expected from the patterning-induced strain relaxation. However it remains positive, which indicates that the dots still have a perpendicular easy axis, which is further proved by the nearly square hysteresis loop measured at the same temperature (Fig. 2). At higher temperature, the reference-pad anisotropy field was found to be proportional to the film magnetization. This result is in agreement with both theoretical predictions based on the mean-field theory[23] and previous measurements on in-plane magnetized (Ga,Mn)As thin films.[24] In the nanodots array, this determination is more problematic as superparamagnetic effects and small signals lead to a high uncertainty. As a consequence, we suppose that H_{eff} is also proportional to the dot magnetization.

In the nanodot array, we determined the temperature dependence of the normalized remnant magnetization and of the coercive field (Fig. 4). The value of the coercive field for the nanodots at low temperature, $\mu_0 H_C(2\text{ K})=(95\pm5)$ mT, being close to the effective anisotropy field, $\mu_0 H_{\text{eff}}(2\text{ K})=109$ mT, we conclude that the magnetization reversal inside the 33-nm-diameter nanodots depicts a quasimacrospin behavior, i.e., a quasicoherent spin-rotation mode if one neglects the low-field reversible behavior. The rounding at low field of the loop at $T=2$ K is assigned to a reversible field-induced rotation of the magnetization inside each nanodot related to a shape-induced nonperfect macrospin behavior (Fig. 2), as checked by minor hysteresis loops. From the vanishing point of $M_R(T)$ and $H_C(T)$, we deduced an experimental blocking temperature, $T_B=(80\pm5)$ K (at a field sweeping rate of 136 mT/s). Note that T_B is significantly smaller than T_C (111 K) for the reference pad, a necessary condition for observing a clear superparamagnetic behavior.

Following Néel and Brown,[1,2] the blocking temperature T_B that determines the onset of the superparamagnetic regime is

$$T_B = K_{\text{eff}} V/k_B \ln(t/\tau_0). \quad (1)$$

Considering the magnetic parameters determined at 80 K ($\mu_0 M_S \approx 8.4$ mT and $K_{\text{eff}} \approx 550$ J/m^3) and using

$\tau_0 = 10^{-9}$ s, we estimate a blocking temperature of (60 ± 20) K (the high uncertainty comes from the volume and anisotropy distribution). This evaluation is consistent with the experimental determination particularly considering that T_B determined on an assembly is generally fixed by the largest nanodots.[25] This agreement further indicates that the magnetization reversal of these nanodots actually occurs by a quasicoherent reversal.

To further prove that the Néel-Brown model applies to these dots, we analyzed the thermal variation in H_C and M_R. Unlike the behavior found for the virgin film or the reference pad, the curvature of the coercive-field thermal dependence is found to be positive in the nanodot array (Fig. 4). In the macrospin model,[26] for H applied along the anisotropy axis, the initial energy barrier is multiplied by $[1-H/H_{\text{eff}}]^2$, i.e., the coercive field can be expressed by the relation

$$H_C = H_{\text{eff}}[1 - \sqrt{k_B T \ln(t/\tau_0)/K_{\text{eff}}V}]. \quad (2)$$

In order to take into account the M_S and K_{eff} temperature dependence as well as the volume and anisotropy distributions to reproduce the H_C and M_R variation, accurate hysteresis loop simulations have been performed, using a rate-equation model based on the macrospin approximation.[25] At each temperature, a rate equation is integrated for each volume and anisotropy constant (note that no correlation has been supposed between both of them) and averaged according to their corresponding distribution. These simulations take into account the same field sweeping rate as in the experiments and can then directly be compared with the experimental results. A good fit is obtained with no additional free parameter as shown in Fig. 4, which further proves the validity of a coherent-reversal model in these nanodots. Note that the slight overestimation of the M_R/M_S ratio is due to the fact that simulations neglect the reversible part observed at low field in the loop at 2 K (see Fig. 2).

Even for a diameter as large as 33 nm, a single-domain behavior for (Ga,Mn)As nanodots is not surprising since the exchange length, $\Lambda = [2A/\mu_0 M_S^2]^{1/2}$ is larger than in metallic systems. A precise estimation of the exchange stiffness, A, is always difficult but reasonable values of A are in the 0.05–0.5 pJ/m range,[18,21] which leads to $12 < \Lambda < 38$ nm at $T=2$ K and $17 < \Lambda < 55$ nm at 80 K. The largest particle size to sustain a single-domain state is given by $D_{\text{max}} \approx \Lambda$, which implies that (Ga,Mn)As nanoparticle must be significantly smaller than 70 nm to be assimilated to a macrospin, a condition that is fulfilled by our $D=33$ nm nanodots. Indeed, in the case of wider nanodots ($D=62$ nm) that have been elaborated together with the previous nanodots, we have measured $H_C/H_{\text{eff}} \approx 0.55$ at 2 K which indicates that they are far from exhibiting a coherent magnetization reversal. Moreover, we never evidenced a net superparamagnetic behavior in these dots, as the temperature at which M_R vanishes (105 K) is too close to the Curie temperature of the reference pad. This is consistent with the fact that, using the magnetic anisotropy measured at 100 K an hypothetical T_B is about 270 K.

IV. CONCLUSION

We have studied the magnetization reversal in nanoelements made from a diluted magnetic semiconductor layer. Although this material is quite sensitive to atomic relaxations and that drastic decrease in magnetic anisotropy could be expected, we have demonstrated that the (33 nm $\times$ 28 nm) cylindrical nanodots still maintain their perpendicular magnetic anisotropy. In spite of the nonconventional nature of ferromagnetism in DMS, the magnetization reversal can be accurately described using a coherent-reversal model. In particular, the characterization of the superparamagnetic transition at 80 K shows a very good agreement with the Néel-Brown model. Indeed, since the exchange length is estimated to about 20–50 nm in (Ga,Mn)As films, single-domain ferromagnetism and superparamagnetic behavior may be studied in nanodots with sizes in the range up to 40 nm, which is not the case for metallic nanostructures. The present results obviously are of great interest for evaluating the performance of future spintronic nanodevices and the development of magnetic random access memories including DMS tunnel junction of very small dimensions.[27]

*rohart@lps.u-psud.fr

[1] L. Néel, Ann. Geophys. (C.N.R.S.) **5**, 99 (1949).
[2] W. Brown, Phys. Rev. **130**, 1677 (1963).
[3] D. Weller and A. Moser, IEEE Trans. Magn. **35**, 4423 (1999).
[4] W. Wernsdorfer, E. B. Orozco, K. Hasselbach, A. Benoit, B. Barbara, N. Demoncy, A. Loiseau, H. Pascard, and D. Mailly, Phys. Rev. Lett. **78**, 1791 (1997).
[5] M. Bode, O. Pietzsch, A. Kubetzka, and R. Wiesendanger, Phys. Rev. Lett. **92**, 067201 (2004).
[6] J. Ferré and J.-P. Jamet, *Handbook of Magnetism and Advanced Materials* (John Wiley & Sons, Chichester, 2007), p. 1710.
[7] M. Lederman, S. Schultz, and M. Ozaki, Phys. Rev. Lett. **73**, 1986 (1994).
[8] W. Coffey, P. Cregg, and Y. Kalmykov, Adv. Chem. Phys. **83**, 263 (1993).
[9] W. Wernsdorfer, E. Bonet Orozco, K. Hasselbach, A. Benoit, D. Mailly, O. Kubo, H. Nakano, and B. Barbara, Phys. Rev. Lett. **79**, 4014 (1997).
[10] S. Wirth, M. Field, D. D. Awschalom, and S. von Molnár, Phys. Rev. B **57**, R14028 (1998).
[11] C. A. Ross, R. Chantrell, M. Hwang, M. Farhoud, T. A. Savas, Y. Hao, H. I. Smith, F. M. Ross, M. Redjdal, and F. B. Humphrey, Phys. Rev. B **62**, 14252 (2000).
[12] O. Fruchart, M. Klaua, J. Barthel, and J. Kirschner, Phys. Rev. Lett. **83**, 2769 (1999).
[13] N. Weiss, T. Cren, M. Epple, S. Rusponi, G. Baudot, S. Rohart, A. Tejeda, V. Repain, S. Rousset, P. Ohresser, F. Scheurer, P. Bencok, and H. Brune, Phys. Rev. Lett. **95**, 157204 (2005).
[14] S. Okamoto, O. Kitakami, N. Kikuchi, T. Miyazaki, Y. Shimada, and Y. K. Takahashi, Phys. Rev. B **67**, 094422 (2003).

[15] T. Jungwirth, K. Y. Wang, J. Mašek, K. W. Edmonds, J. König, J. Sinova, M. Polini, N. A. Goncharuk, A. H. MacDonald, M. Sawicki, A. W. Rushforth, R. P. Campion, L. X. Zhao, C. T. Foxon, and B. L. Gallagher, Phys. Rev. B **72**, 165204 (2005).
[16] S. P. Bennett and D. Heiman, J. Appl. Phys. **104**, 024309 (2008).
[17] L. Thevenard, L. Largeau, O. Mauguin, G. Patriarche, A. Lemaître, N. Vernier, and J. Ferré, Phys. Rev. B **73**, 195331 (2006).
[18] T. Dietl, H. Ohno, and F. Matsukura, Phys. Rev. B **63**, 195205 (2001).
[19] Available at http://www.comsol.com
[20] G. V. Astakhov, H. Hoffmann, V. L. Korenev, T. Kiessling, J. Schwittek, G. M. Schott, C. Gould, W. Ossau, K. Brunner, and L. W. Molenkamp, Phys. Rev. Lett. **102**, 187401 (2009).
[21] C. Gourdon, A. Dourlat, V. Jeudy, K. Khazen, H. J. von Bardeleben, L. Thevenard, and A. Lemaître, Phys. Rev. B **76**, 241301(R) (2007).
[22] V. Grolier, J. Ferré, A. Maziewski, E. Stefanowicz, and D. Renard, J. Appl. Phys. **73**, 5939 (1993).
[23] T. Dietl, J. König, and A. H. MacDonald, Phys. Rev. B **64**, 241201(R) (2001).
[24] K.-Y. Wang, M. Sawicki, K. W. Edmonds, R. P. Campion, S. Maat, C. T. Foxon, B. L. Gallagher, and T. Dietl, Phys. Rev. Lett. **95**, 217204 (2005).
[25] S. Rohart, V. Repain, A. Tejeda, P. Ohresser, F. Scheurer, P. Bencok, J. Ferré, and S. Rousset, Phys. Rev. B **73**, 165412 (2006).
[26] O. Fruchart and A. Thiaville, C. R. Phys. **6**, 921 (2005).
[27] M. Elsen, H. Jaffrès, R. Mattana, M. Tran, J.-M. George, A. Miard, and A. Lemaître, Phys. Rev. Lett. **99**, 127203 (2007).